ADAPTIVE CONTROL OF A TILT-ROTOR UAV IN LOAD TRANSPORTATION TASKS - A LMI BASED APPROACH

Marcelo Alves dos Santos*, Guilherme Vianna Raffo*†

*Graduate Program in Electrical Engineering - Federal University of Minas Gerais
Av. Antônio Carlos 6627, 31270-901, Belo Horizonte, MG, Brazil

†Department of Electronic Engineering - Federal University of Minas Gerais
Av. Antônio Carlos 6627, 31270-901, Belo Horizonte, MG, Brazil

Emails: cidomg32@ufmg.br, raffo@ufmg.br

Abstract— This paper proposes an adaptive control strategy to solve the path tracking problem of a Tilt-rotor UAV in load transportation tasks. Initially, a nonlinear dynamic model is obtained through the Euler-Lagrange formulation and linearized around a reference trajectory in order to obtain a linear parameter-varying model. Therefore, a discrete linear adaptive controller based on the LMI approach is designed to ensure closed-loop stability and increase the system's domain of attraction. In addiction, simulation results are shown to verify the good performance of the proposed controller in presence of external disturbances and model uncertainties.

Keywords— Adaptive Control, Load Transportation, UAV, LMI, Underactuated Mechanical System

Resumo— Esse artigo propõe uma estratégia de controle adaptativo para resolver o problema de rastreamento de trajetória para um VANT Tilt-rotor utilizado para o transporte de carga. Inicialmente, um modelo dinâmico não linear é obtido via formulação de Euler-Lagrange e linearizado em torno de uma trajetória de referência para se obter um modelo linear a parâmetros variantes. Através do modelo obtido, um controlador adaptativo discreto baseado na abordagem de LMIs é projetado a fim de garantir estabilidade em malha fechada e de aumentar o domínio de atração do sistema. Adicionalmente, resultados de simulação são apresentados para verificar o bom desempenho do controlador proposto na presença de perturbações externas e incertezas de modelo.

Palavras-chave— Controle Adaptativo, Transporte de Carga, VANT, LMI, Sistema Mecânico Subatuado.

1 Introduction

The several possibilities for UAVs applications as well the issues related to the development of these vehicles has attracted the attention of the academia in the last two decades. Some examples of applications are: precision agriculture, aerial surveillance, and load transportation.

UAVs are mainly presented in two regular configurations: rotary-wing and fixed-wing. The rotary-wing aircraft has the ability to take-off and landing vertically, while the fixed-wing one can reach high cruising speeds. Seeking to combine these abilities, the Tilt-rotor structure was proposed. This kind of aircraft is particularly interesting to perform tasks that require fast deployment and access to restricted areas, for example, search and rescue and cargo transportation.

Tilt-rotor UAVs are underactuated mechanical systems since it has more degrees of freedom (DOF) than actuators. This means that is not possible to control all DOF at the same instant of time. Hence, the path tracking control problem must be formulated for tracking some desired DOF while the remaining ones are kept stable. The tiltable mechanisms that allows the thrusters' motion, increases the mechanical complexity, when compared with others UAVs. Furthermore, the system model is nonlinear and could become non-affine at the inputs depending on how the control inputs are selected. All these features result in a more complex system modeling leading to a challenging control design.

Researches dealing with control design for Tilt-rotors UAVs are recent with few works published in the literature. Some relevant works have used the follow control techniques: model predictive (Papachristos et al., 2013); back-stepping (Amiri et al., 2013); and robust linear (Donadel et al., 2014). On the other hand, only Almeida and Raffo (2015) addresses the load transportation problem considering a Tilt-rotor UAV. Although, if different UAVs structures are considered, many works dealing with the load transportation control problem can be found in the literature (Sreenath et al., 2013; Faust et al., 2013).

Generally, aerial vehicles presents highly nonlinear dynamic behavior, making linear controllers based on the nominal linearized model unsuitable to perform flight control even in a limited operating range. Gain-scheduled controllers are a technique widely used to obtain a system with higher domain of attraction and then overcome this issue. However, in some frameworks it is not trivial to ensure stability for the global system controlled by a gain-scheduled controller.

Therefore, this paper presents a discrete linear adaptive controller designed to perform path tracking of a Tilt-rotor UAV at the rotary-wing flight mode while carrying a suspended load stably. The adaptive control law schedule the feedback gain using an optimal convex combination of individual gains obtained using a polytopic representation to describe the nonlinear system as an uncertain linear system.

2 System Model

This section briefly describes the equations of motion for a Tilt-rotor UAV with suspended load through the Euler-Lagrange formulation. More details about the model formulation can be found on Almeida and Raffo (2015).

The complete system can be seen as a multi-body system: the Tilt-rotor UAV composed by three bodies (a main body and two thrusters' groups) and the suspended load being the fourth body. For modeling purposes, all bodies are assumed rigid and the load is assumed to be attached to the main body by a massless inelastic rod on a spherical joint. Moreover, each thruster's group is composed by a rotor to generate the lift force and a servomotor to tilt the propellers.

Six frames are defined to describe the Tilt-rotor UAV motion: the inertial frame $\mathcal{I}$, and the moving frames $\mathcal{B}$ and $\mathcal{C}_i$, which are, respectively, frames rigidly attached to the main body and the center of mass of the i-th body (see Fig. 1).

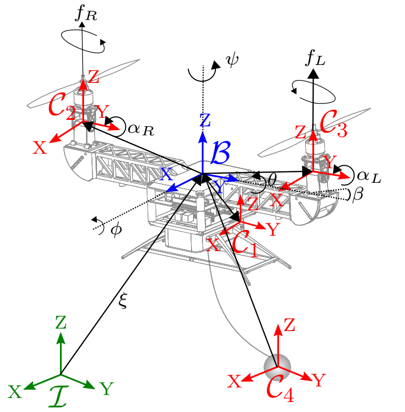

Fig. 1: Frames and variables definition.

The position of the body frame's origin represented in the inertial frame is given by $\boldsymbol{\xi} = [x\ y\ z]'$, and the attitude by $\boldsymbol{\eta} = [\phi\ \theta\ \psi]'$, described by Euler angles using the ZYX convention about local axes. The orientation of $\mathcal{C}_2$ with respect to $\mathcal{B}$ is obtained by a rotation α_R around the $\mathrm{Y}^{\mathcal{B}}$-axis and a constant negative tilt angle β around the $\mathrm{X}^{\mathcal{B}}$-axis. Likewise, the rotation of the frame $\mathcal{C}_3$ with respect to $\mathcal{B}$ can be obtained considering rotations α_L around the $\mathrm{Y}^{\mathcal{B}}$-axis and a constant tilt angle β around the $\mathrm{X}^{\mathcal{B}}$-axis. Further, using a parametrization that considers the load as a pendulum with length l and two degrees of freedom represented by γ_1 and γ_2 (rotations around $\mathrm{X}^{\mathcal{B}}$-axis and $\mathrm{Y}^{\mathcal{B}}$-axis, respectively); the position of the suspended load with respect to the main body becomes a simple forward kinematic problem.

Therefore, the generalized coordinates that describe the motion of the Tilt-rotor UAV are defined as $\boldsymbol{q} = [\boldsymbol{\xi}'\ \boldsymbol{\eta}'\ \alpha_R\ \alpha_L\ \gamma_1\ \gamma_2]'$. Furthermore, the system's inputs are given by $\boldsymbol{u} = [f_R\ f_L\ \tau_R\ \tau_L]'$, were f_R and f_L are the thrust forces of the right and left propellers, respectively; likewise, τ_R and τ_L are the torques applied by the servomotors.

2.1 Dynamic Model

The nonlinear dynamic model of the Tilt-rotor UAV with suspended load can be described by the Euler-Lagrange equations as:

$$\boldsymbol{M}\ddot{\boldsymbol{q}} + \boldsymbol{C}\dot{\boldsymbol{q}} + \boldsymbol{G} = \boldsymbol{F} + \boldsymbol{F}_{drag} + \boldsymbol{F}_{ext}, \tag{1}$$

where $\boldsymbol{M} \triangleq \boldsymbol{M}(\boldsymbol{q}) \in \mathbb{R}^{10\times 10}$ is the inertia matrix, $\boldsymbol{C} \triangleq \boldsymbol{C}(\boldsymbol{q}, \dot{\boldsymbol{q}}) \in \mathbb{R}^{10\times 10}$ is the Coriolis and centripetal forces matrix, $\boldsymbol{G} \triangleq \boldsymbol{G}(\boldsymbol{q}) \in \mathbb{R}^{10}$ is the gravitational force vector, $\boldsymbol{F} \triangleq \boldsymbol{F}(\boldsymbol{q}) \in \mathbb{R}^{10}$ is the generalized input force and torque vector, $\boldsymbol{F}_{drag} \in \mathbb{R}^{10}$ is the generalized *drag force* vector and the vector $\boldsymbol{F}_{ext} \in \mathbb{R}^{10}$ represents the external disturbances acting on the generalized coordinates.

Assuming that the drag forces are proportional to the generalized velocity, $\boldsymbol{F}_{drag} = -\boldsymbol{\mu}\dot{\boldsymbol{q}}$, the equation (1) can be rewritten as:

$$\boldsymbol{M}\ddot{\boldsymbol{q}} + [\boldsymbol{C} + \boldsymbol{\mu}]\,\dot{\boldsymbol{q}} + \boldsymbol{G} = \boldsymbol{F} + \boldsymbol{F}_{ext}, \tag{2}$$

where $\boldsymbol{\mu}$ is a constant diagonal matrix.

Taking the generalized positions and velocities as states, i.e. $\boldsymbol{x} = [\boldsymbol{q}'\ \dot{\boldsymbol{q}}']'$, the equation (2) can be written in a state-space representation as:

$$\dot{\boldsymbol{x}} = \begin{bmatrix} \dot{\boldsymbol{q}} \\ \boldsymbol{M}^{-1}\left[\boldsymbol{B}\boldsymbol{u} + \boldsymbol{d} - [\boldsymbol{C} + \boldsymbol{\mu}]\,\dot{\boldsymbol{q}} - \boldsymbol{G}\right] \end{bmatrix}, \tag{3}$$

where $\boldsymbol{d} = \boldsymbol{F_{ext}}$, and $\boldsymbol{F} = \boldsymbol{B}\boldsymbol{u}$; being $\boldsymbol{B} \triangleq \boldsymbol{B}(\boldsymbol{q}) \in \mathbb{R}^{10\times 4}$ a jacobian that maps the input forces in the inertial frame.

2.2 Linearized Model

Once this work addresses the path tracking problem through a linear control strategy, the state-space model (3) must be linearized around a reference trajectory. Therefore, consider the vehicle in hovering without any external disturbances ($\boldsymbol{d} = \boldsymbol{0}$). The equilibrium points can be obtained after solving $\dot{\boldsymbol{x}} = \boldsymbol{f}(\bar{\boldsymbol{x}}, \bar{\boldsymbol{u}}, t) = \boldsymbol{0}$, leading to the system of algebraic equations $\boldsymbol{B}(\bar{\boldsymbol{q}})\,\bar{\boldsymbol{u}} - \boldsymbol{G}(\bar{\boldsymbol{q}}) = \boldsymbol{0}$, where $(\bar{\cdot})$ denotes the equilibrium.

Nevertheless, this algebraic system has more variables than equations meaning that an infinity set of real numbers can solve the problem. To overcome this issue, let the states x, y and z assume any value along the trajectory and let $\psi = 0$. Thus, the equilibrium values for the states and system inputs can be obtained. The reference trajectory can be expressed as $\boldsymbol{x}_r(t) = [\boldsymbol{q}_r'\ \dot{\boldsymbol{q}}_r'] = \left[x_r\ y_r\ z_r\ \bar{\phi}\ \bar{\theta}\ 0\ \bar{\alpha}_R\ \bar{\alpha}_L\ \bar{\gamma}_1\ \bar{\gamma}_2\ \dot{x}_r\ \dot{y}_r\ \dot{z}_r\ 0\ 0\ 0\ 0\ 0\ 0\ 0\right]'$.

Likewise, rearranging (2) and evaluating at reference trajectory, it is possible to express the reference control signal as $\boldsymbol{u}_r(t) = \boldsymbol{B}^{+}(\boldsymbol{q}_r)\left[\boldsymbol{M}(\boldsymbol{q}_r)\ddot{\boldsymbol{q}}_r + [\boldsymbol{C}(\boldsymbol{q}_r, \dot{\boldsymbol{q}}_r) + \boldsymbol{\mu}]\,\dot{\boldsymbol{q}}_r + \boldsymbol{G}(\boldsymbol{q}_r)\right]$, being $(\cdot)^{+}$ the Moore-Penrose pseudoinverse.

Finally, the linearized model can be obtained:

$$\Delta\dot{\boldsymbol{x}} = \boldsymbol{A}(t)\Delta\boldsymbol{x} + \boldsymbol{B}(t)\Delta\boldsymbol{u}, \tag{4}$$

where $\Delta\boldsymbol{x} = \boldsymbol{x} - \boldsymbol{x}_r$, $\Delta\boldsymbol{u} = \boldsymbol{u} - \boldsymbol{u}_r$, and:

$$\boldsymbol{A}(t) = \frac{\partial \boldsymbol{f}(\boldsymbol{x}, \boldsymbol{u}, t)}{\partial \boldsymbol{x}}\Big|_{\substack{\boldsymbol{u}=\boldsymbol{u}_r \\ \boldsymbol{x}=\boldsymbol{x}_r}}, \quad \boldsymbol{B}(t) = \frac{\partial \boldsymbol{f}(\boldsymbol{x}, \boldsymbol{u}, t)}{\partial \boldsymbol{u}}\Big|_{\substack{\boldsymbol{u}=\boldsymbol{u}_r \\ \boldsymbol{x}=\boldsymbol{x}_r}}.$$

ISSN 2525-8311

2.3 Uncertain Linear Model

After solve the partial derivatives it turns out that $\boldsymbol{A}(t) \in \mathbb{R}^{20\times 20}$ is a function of $\ddot{x}_r$, $\ddot{y}_r$, and $\ddot{z}_r$, and $\boldsymbol{B}(t) \in \mathbb{R}^{20\times 4}$ is a constant matrix. Thus, the linear parameter-varying model obtained in (4) can be written as $\Delta\dot{\boldsymbol{x}} = \boldsymbol{A}(\ddot{x}_r(t), \ddot{y}_r(t), \ddot{z}_r(t))\Delta\boldsymbol{x} + \boldsymbol{B}\Delta\boldsymbol{u}$.

Considering the reference accelerations $\ddot{x}_r$, $\ddot{y}_r$, and $\ddot{z}_r$ as bounded uncertainties, the uncertain linear model can be expressed in the polytopic form:

$$\boldsymbol{A}(\boldsymbol{\alpha}) = \boldsymbol{A}(\ddot{x}_r(t), \ddot{y}_r(t), \ddot{z}_r(t)) = \sum_{i=1}^{N} \alpha_i \boldsymbol{A}_i, \qquad (5)$$
$$s.t. \sum_{i=1}^{N} \alpha_i = 1,\ \alpha_i \geq 0,\ \forall i = 1, \cdots, N,$$

where $\boldsymbol{\alpha} \in \Delta$ is a vector of uncertain parameters and Δ is a polytope with 2^3 vertices. Thus, the uncertain linear model can be written as:

$$\Delta\dot{\boldsymbol{x}} = \boldsymbol{A}(\boldsymbol{\alpha})\Delta\boldsymbol{x} + \boldsymbol{B}\Delta\boldsymbol{u},\ s.t. \begin{cases} \ddot{x}_r^{min} \leq \ddot{x}_r(t) \leq \ddot{x}_r^{max}, \\ \ddot{y}_r^{min} \leq \ddot{y}_r(t) \leq \ddot{y}_r^{max}, \\ \ddot{z}_r^{min} \leq \ddot{z}_r(t) \leq \ddot{z}_r^{max}. \end{cases}$$

2.4 Integral Action

In order to perform path tracking with null steady-state error when constant disturbances affect the system, integral action acting on some desired states must be considered. In this work the integral action is applied to x, y, z, and ψ.

Consider the vector $\boldsymbol{\epsilon} = [x - x_r\ \ y - y_r\ \ z - z_r\ \ \psi - \psi_r]'$. Adding to the state vector the integral of $\boldsymbol{\epsilon}$, it is possible to obtain integral action. Thus, the new state-space model is given by:

$$\begin{bmatrix} \Delta\dot{\boldsymbol{x}}(t) \\ \boldsymbol{\epsilon}(t) \end{bmatrix} = \left[\begin{array}{cccccc|c} \multicolumn{6}{c|}{\boldsymbol{A}(\boldsymbol{\alpha})} & \boldsymbol{0} \\ \hline 1 & 0 & 0 & 0 & 0 & 0 & \\ 0 & 1 & 0 & 0 & 0 & 0 & \boldsymbol{0} \\ 0 & 0 & 1 & 0 & 0 & 0 & \\ 0 & 0 & 0 & 0 & 0 & 1 & \end{array}\right] \begin{bmatrix} \Delta\boldsymbol{x}(t) \\ \int \boldsymbol{\epsilon}(t) \end{bmatrix} + \begin{bmatrix} \boldsymbol{B} \\ \boldsymbol{0} \end{bmatrix} \Delta\boldsymbol{u}(t),$$

where $\boldsymbol{0}$ is a zero matrix with appropriate dimension. Therefore, the augmented state-space can be rewritten in a compact form as[1]:

$$\Delta\dot{\boldsymbol{x}} = \hat{\boldsymbol{A}}(\boldsymbol{\alpha})\Delta\boldsymbol{x} + \hat{\boldsymbol{B}}\Delta\boldsymbol{u}. \qquad (6)$$

Since a discrete controller will be considered, it is necessary to map (6) from the continuous time to the discrete time domain, leading to $\Delta\boldsymbol{x}_{k+1} = \hat{\boldsymbol{A}}_d(\boldsymbol{\alpha})\Delta\boldsymbol{x}_k + \hat{\boldsymbol{B}}_d\Delta\boldsymbol{u}_k$, where the matrices $\hat{\boldsymbol{A}}_d(\boldsymbol{\alpha})$ and $\hat{\boldsymbol{B}}_d$ are obtained after discretize the model using a zero-order hold with sample time T.

3 Adaptive Controller

This section deals with the problem of designing a controller able of solving the path tracking problem for a Tilt-rotor UAV. The main objectives are to ensure stability for the closed-loop system and reject constant external disturbances and modeling uncertainties. The controller developed in this work is based on Gonzalez et al. (2010).

[1]The reader should note that, for the sake of simplicity, the symbol $(\hat{\cdot})$ was omitted in (6). Thus, for now on, $\Delta\boldsymbol{x}$ will represent the extended state vector.

3.1 Control Problem Formulation

An adaptive control law that reach the proposed objectives can be defined as $\Delta\boldsymbol{u}_k = \boldsymbol{K}(\boldsymbol{\alpha})\Delta\boldsymbol{x}_k$, where the feedback gain is defined as a convex combination of each individual feedback gain calculated for each vertex of the polytope, that is:

$$\boldsymbol{K}(\boldsymbol{\alpha}) \triangleq \alpha_1\boldsymbol{K}_1 + \alpha_2\boldsymbol{K}_2 + \cdots + \alpha_N\boldsymbol{K}_N. \qquad (7)$$

Consider the error model given by $\Delta\boldsymbol{x}_{k+1} = (\hat{\boldsymbol{A}}_d(\boldsymbol{\alpha}) + \hat{\boldsymbol{B}}_d\boldsymbol{K}(\boldsymbol{\alpha}))\Delta\boldsymbol{x}_k$, the goal is to obtain $\boldsymbol{K}(\boldsymbol{\alpha})$ that ensures asymptotic stability and reach some performance specification.

Therefore, consider the following Lyapunov function $V(\Delta\boldsymbol{x}_k) = \Delta\boldsymbol{x}_k'\lambda\boldsymbol{P}\Delta\boldsymbol{x}_k$, where $\lambda \in \mathbb{R}^+$ is a scaling factor. In order to obtain an asymptotically stable system, the conditions $\boldsymbol{P} > 0$ and $V(\Delta\boldsymbol{x}_{k+1}) - V(\Delta\boldsymbol{x}_k) < 0$ must be satisfied.

Aiming to add some performance requirements to the problem, $V(\Delta\boldsymbol{x}_k)$ is considered as an upper bound for the linear quadratic regulator (LQR) cost function. Thereby, the closed-loop system dynamics with an adaptive control law should be as close from the LQR controller performance as the optimization problem achieve. Therefore, the following problem is considered:

$$V(\Delta\boldsymbol{x}_0) \geq \min_{u[0,\infty)} \sum_{k=0}^{\infty} \Delta\boldsymbol{x}_k'\boldsymbol{Q}\Delta\boldsymbol{x}_k + \Delta\boldsymbol{u}_k'\boldsymbol{R}\Delta\boldsymbol{u}_k. \qquad (8)$$

To obtain some valid linear matrix inequalities (LMI) conditions through (8), consider as necessary condition to asymptotic stability and performance the inequality below:

$$\begin{aligned} &\Delta\boldsymbol{x}_k' \left(\hat{\boldsymbol{A}}_f'\lambda\boldsymbol{P}\hat{\boldsymbol{A}}_f\right)\Delta\boldsymbol{x}_k - \Delta\boldsymbol{x}_k'(\lambda\boldsymbol{P})\Delta\boldsymbol{x}_k \\ &\quad \leq -\Delta\boldsymbol{x}_k'\left(\boldsymbol{Q} + \boldsymbol{K}'(\boldsymbol{\alpha})\boldsymbol{R}\boldsymbol{K}(\boldsymbol{\alpha})\right)\Delta\boldsymbol{x}_k, \end{aligned} \qquad (9)$$

where $\hat{\boldsymbol{A}}_f = \hat{\boldsymbol{A}}_d(\boldsymbol{\alpha}) + \hat{\boldsymbol{B}}_d\boldsymbol{K}(\boldsymbol{\alpha})$.

Since (9) is not a valid LMI condition, the inequality needs to be manipulated. Hence, rearranging (9) and applying the Schur complement twice (Álamo et al., 2006), it holds that:

$$\begin{bmatrix} \boldsymbol{P} & \hat{\boldsymbol{A}}_f' & \boldsymbol{Q}^{\frac{1}{2}} & \boldsymbol{K}'(\boldsymbol{\alpha})\boldsymbol{R}^{\frac{1}{2}} \\ \hat{\boldsymbol{A}}_f & \boldsymbol{P}^{-1} & \boldsymbol{0} & \boldsymbol{0} \\ \boldsymbol{Q}^{\frac{1}{2}} & \boldsymbol{0} & \lambda\boldsymbol{I} & \boldsymbol{0} \\ \boldsymbol{R}^{\frac{1}{2}}\boldsymbol{K}(\boldsymbol{\alpha}) & \boldsymbol{0} & \boldsymbol{0} & \lambda\boldsymbol{I} \end{bmatrix} \geq 0. \qquad (10)$$

In order to remove the nonlinear terms, it is necessary to pre and post multiply (10) by the block diagonal matrix $\mathbf{blkdiag}\left(\boldsymbol{P}^{-1}, \boldsymbol{I}, \boldsymbol{I}, \boldsymbol{I}\right)$, and to define $\boldsymbol{S} = \boldsymbol{P}^{-1}$, $\boldsymbol{Y}(\boldsymbol{\alpha}) = \boldsymbol{K}(\boldsymbol{\alpha})\boldsymbol{P}^{-1}$.

Thus, the LMI condition used to calculate a state feedback controller that ensure stability and performance to the uncertain system can be written as:

$$\begin{bmatrix} \boldsymbol{S} & \boldsymbol{H}' & \boldsymbol{S}\boldsymbol{Q}^{\frac{1}{2}} & \boldsymbol{Y}'(\boldsymbol{\alpha})\boldsymbol{R}^{\frac{1}{2}} \\ \boldsymbol{H} & \boldsymbol{S} & \boldsymbol{0} & \boldsymbol{0} \\ \boldsymbol{Q}^{\frac{1}{2}}\boldsymbol{S} & \boldsymbol{0} & \lambda\boldsymbol{I} & \boldsymbol{0} \\ \boldsymbol{R}^{\frac{1}{2}}\boldsymbol{Y}(\boldsymbol{\alpha}) & \boldsymbol{0} & \boldsymbol{0} & \lambda\boldsymbol{I} \end{bmatrix} \geq 0. \qquad (11)$$

where $\boldsymbol{H} = \hat{\boldsymbol{A}}_d(\boldsymbol{\alpha})\boldsymbol{S} + \hat{\boldsymbol{B}}_d\boldsymbol{Y}(\boldsymbol{\alpha})$.

Likewise, it is possible to obtain a LMI condition to constrain the control signal amplitude.

However, first it is needed to map the control signal amplitude to the maximum increment of control.

Consider the upper and lower admissible control signals, respectively, $\boldsymbol{u}^{up}$ and $\boldsymbol{u}^{lb}$; the maximum increment of control can be defined as $\Delta\boldsymbol{u}^m \triangleq min\left(\boldsymbol{u}_r - \boldsymbol{u}^{lb}, \boldsymbol{u}^{up} - \boldsymbol{u}_r\right)$. Then, the LMI condition can be obtained by solving:

$$\Delta\boldsymbol{u}_k = \boldsymbol{K}(\boldsymbol{\alpha})\Delta\boldsymbol{x}_k < \Delta\boldsymbol{u}^m. \tag{12}$$

Considering also the problem to determinate the maximum value of a linear function with ellipsoidal constraints (Álamo et al., 2006) as follows:

$$a^* = \underset{\Delta\boldsymbol{x}_k}{max}\ \boldsymbol{K}(\boldsymbol{\alpha})\Delta\boldsymbol{x}_k,\ \ s.t\ \Delta\boldsymbol{x}_k'\boldsymbol{P}\Delta\boldsymbol{x}_k \leq 1, \tag{13}$$

for which the solution is given by:

$$a^* = \sqrt{\boldsymbol{K}(\boldsymbol{\alpha})\boldsymbol{P}^{-1}\boldsymbol{K}'(\boldsymbol{\alpha})}. \tag{14}$$

Thus, a sufficient condition to solve (12) is:

$$\boldsymbol{K}(\boldsymbol{\alpha})\boldsymbol{P}^{-1}\boldsymbol{K}'(\boldsymbol{\alpha}) < (\Delta\boldsymbol{u}^m)^2. \tag{15}$$

The LMI condition to constrain the control signal amplitude is obtained rearranging (15) and applying the Schur's complement, which yields to:

$$\begin{bmatrix} (\Delta\boldsymbol{u}^m)^2 & \boldsymbol{Y}(\boldsymbol{\alpha}) \\ \boldsymbol{Y}'(\boldsymbol{\alpha}) & \boldsymbol{S} \end{bmatrix} > 0. \tag{16}$$

In addition a LMI condition is used to constrain the maximum states error as:

$$|\boldsymbol{e}| < \left[e_x^m\ e_y^m\ e_z^m\ e_\phi^m\ e_\theta^m\ e_\psi^m\ e_{\alpha_R}^m\ e_{\alpha_L}^m\ e_{\gamma_1}^m\ e_{\gamma_2}^m\right]', \tag{17}$$

where e_i^m is the maximum error for the *i-th* state.

The inequality (17) can be rewritten as:

$$|\boldsymbol{f}_i\boldsymbol{e}| < e_i^m, \tag{18}$$

where $\boldsymbol{f}_1 = [1\ 0\ \cdots\ 0]'$, $\boldsymbol{f}_2 = [0\ 1\ \cdots\ 0]'$, and so on.

Consider again the problem of obtain the maximum value of a function with ellipsoidal constraints presented in (13) and (14). Using the same procedure as in (15), inequality (18) can be written by the following LMI:

$$\boldsymbol{f}_i\boldsymbol{S}\boldsymbol{f}_i' < (e_i^{max})^2,\quad \forall i = 1, \cdots, 10. \tag{19}$$

3.2 Adaptive Control Law

After finding a feasible solution to the LMIs presented in (11), (16), and (19), feedback gains $\boldsymbol{K}_1, \cdots, \boldsymbol{K}_8$ are obtained. The feedback gain $\boldsymbol{K}(\boldsymbol{\alpha})$ is a convex combination, as defined in (7), and the coefficients α_i are obtained solving a linear optimization problem.

Consider the cost function:

$$\mathcal{J} = tr\left((\alpha_1\boldsymbol{A}_1 + \cdots + \alpha_8\boldsymbol{A}_8)\hat{\boldsymbol{A}}_\alpha^{-1} - \boldsymbol{I}\right), \tag{20}$$

where $tr(\cdot)$ is the trace operator, and $\hat{\boldsymbol{A}}_\alpha$ is the current realization of the system. Using the trace properties, (20) can be rewritten in the canonical linear form as $\mathcal{J} = \boldsymbol{f}'\boldsymbol{\alpha} + f_0$, where:

$$\boldsymbol{f}' = \left[tr\left(\boldsymbol{A}_1\hat{\boldsymbol{A}}_\alpha^{-1}\right)\ tr\left(\boldsymbol{A}_2\hat{\boldsymbol{A}}_\alpha^{-1}\right)\ \cdots\ tr\left(\boldsymbol{A}_8\hat{\boldsymbol{A}}_\alpha^{-1}\right)\right],$$
$$f_0 = -tr\left(\boldsymbol{I}\right).$$

Adding the constraints presented in (5), the following optimization problem must be solved in order to obtain the $\boldsymbol{\alpha}$ vector:

$$\min_{\boldsymbol{\alpha}}\ \boldsymbol{f}'\boldsymbol{\alpha},\quad s.t\left\{\begin{array}{l} \sum\alpha = 1, \\ \alpha \geq 0. \end{array}\right. \tag{21}$$

4 Simulation Results

This section presents the simulation results obtained by applying the proposed adaptive controller to perform path tracking of the Tilt-rotor UAV carrying a suspended load. Since the system is underactuated, only x, y, z, and ψ are tracked, and the remaining DOF are stabilized around their equilibrium points.

The discrete linear model used for controller design purposes is obtained with sampling time $T = 12\ ms$, which is chosen regarding the hardware and actuators features. The maximum absolute acceleration for x, y, and z is 2.5 m/s^2. The propellers can deliver thrusts in the region $0 \leq f_R, f_L \leq 30$ N and the servomotors are able to apply torque $-2 \leq \tau_R, \tau_L \leq 2$ N.m. Further, the maximum state error considered in (19) is $\boldsymbol{e} = [1\ 1\ 1\ 1\ 1\ 1\ 1\ 1\ 0.5\ 0.5]$, where the linear error is given in meters and the angular error in radians.

The system physical parameters are: the distance between the frames $\mathcal{B}$ and $\mathcal{C}_i$ given in meters by $\boldsymbol{d}_1^{\mathcal{B}} = [-0.00433\ 0.00060\ -0.04559]$, $\boldsymbol{d}_2^{\mathcal{B}} = [-0.00002\ -0.27761\ 0.05493]$, $\boldsymbol{d}_3^{\mathcal{B}} = [0.00077\ 0.27761\ 0.05493]$; the mass of the *i-th* body given in kg by $m_1 = 1.70249$, $m_2 = m_3 = 0.13973$, $m_4 = 0.050$; the gravitational acceleration $g = 9.81\ m/s^2$; the aerodynamic constant $k_d = 0.01789\ m$; the propellers' tilt angle $\beta = 5°$; the length of the rod attaching the load to the vehicle $l = 0.5\ m$; the viscous friction constant $\boldsymbol{\mu} = diag(0, 0, 0, 0, 0, 0, 0, 0, 0.005, 0.005)\ N/m^2$; and the inertia moment of the *i-th* body in relation to the axes j and k, I_{jk}^i, given in $kg.m^2$ by $I_{xx}^1 = 0.00369766749$, $I_{yy}^1 = 0.00084010403$, $I_{zz}^1 = 0.00386505354$, $I_{xy}^1 = 0.00000036342$, $I_{xz}^1 = -0.00000951029$, $I_{yz}^1 = 0.00000061804$, $I_{xx}^2 = I_{xx}^3 = 0.00044168245$, $I_{yy}^2 = I_{yy}^3 = 0.00044167985$, $I_{zz}^2 = I_{zz}^3 = 0.00000064418$, $I_{xy}^2 = I_{xy}^3 = 0$, $I_{xz}^2 = -I_{xz}^3 = -0.00000000026$, $I_{yz}^2 = -I_{yz}^3 = -0.00000107006$, $I_{xx}^4 = I_{yy}^4 = I_{zz}^4 = 0.000002645$.

The equilibrium values for the linear system are $\bar{\phi} = -0.00016$ rad, $\bar{\theta} = -0.04180$ rad, $\bar{\alpha}_R = 0.04176$ rad, $\bar{\alpha}_L = 0.04153$ rad, $\bar{\gamma}_1 = 0.00016$ rad, $\bar{\gamma}_2 = 0.04180$ rad, $\bar{f}_R = 9.98680$ N, $\bar{f}_L = 10.02264$ N, $\bar{\tau}_R = 0$ N.m, and $\bar{\tau}_L = 0$ N.m.

The weighting matrices $\boldsymbol{Q}$ and $\boldsymbol{R}$ are obtained using the Bryson's method as an initial tune (Johnson and Grimble, 1987), followed by a fine adjustment in order to obtain a good path tracking performance. The used values are:

$$\text{diag}\left(\boldsymbol{r}_i\right) = \left(\frac{10}{(\bar{f}_R)^2}, \frac{10}{(\bar{f}_L)^2}, \frac{5}{(2-\bar{\tau}_R)^2}, \frac{5}{(2-\bar{\tau}_L)^2}\right).$$

$$\operatorname{diag}(\boldsymbol{q}_i) = \Big(1, 1, 1, \frac{1}{(\frac{\pi}{2})^2}, \frac{1}{(\frac{\pi}{2})^2}, \frac{1}{(\frac{\pi}{2})^2}, \frac{0.1}{(\frac{\pi}{2})^2}, \frac{0.1}{(\frac{\pi}{2})^2}, \frac{10}{(\frac{\pi}{2})^2}, \frac{10}{(\frac{\pi}{2})^2}, \frac{1}{2^2}, \frac{1}{2^2}, \frac{1}{2^2}, \frac{1}{(3\pi)^2}, \frac{1}{(3\pi)^2}, \frac{1}{(3\pi)^2}, \frac{0.09}{(3\pi)^2}, \frac{0.09}{(3\pi)^2}, \frac{1}{(3\pi)^2}, \frac{1}{(3\pi)^2}, 20, 20, 20, 10\Big),$$

The problem of finding a feasible solution to the LMIs presented in (11), (16), and (19) is solved using the YALMIP solver. Also, the optimization problem (21) is solved using the MATLAB's *linprog* solver with an interior-point algorithm.

In order to analyze the proposed controller, a LQR controller is designed to compare the system's closed-loop response in two different simulation scenarios. The LQR controller is obtained using the same $\boldsymbol{Q}$ and $\boldsymbol{R}$ matrices proposed above.

4.1 Scenario 1

In this scenario, the ability of the proposed controller to reject constant disturbances is tested while tracking a reference with low accelerations. The reference trajectory is given by: $x = 1.25\cos((\pi/50)t)$, $y = 1.25\sin((\pi/50)t)$, $z = 3.5 - 2.5\cos((\pi/50)t)$, and $\psi = 0$. The system undergoes the external disturbances shown in Table 1.

Fig. 2 shows the 3D trajectory of the Tilt-rotor UAV and Fig. 3-6 show the system's DOF. Observe that the proposed controller was able to track the desired trajectory and keep the remaining DOF stable around the equilibria. Although in Fig. 4-6 the system stabilizes in equilibrium values distinct from those presented in this section, it should be noted that the disturbances makes the equilibria changes over time. In addition, Fig. 7 shows the control input applied to the system.

The table 2 shows the mean squared error (MSE) and the integral of absolute value of the control derivative (IADU) to compare the proposed controller and the LQR. Clearly, the LQR controller presents better performance with less control effort. This is expected once the system, even in the presence of disturbance, stays near to the nominal system, i.e., the system considering null accelerations.

F_x^{ext}	F_y^{ext}	F_z^{ext}	F_ϕ^{ext}	F_θ^{ext}
1 N	1 N	1 N	0.1 N.m	0.1 N.m
$t > 10$ s	$t > 18$ s	$t > 26$ s	$t > 34$ s	$t > 42$ s
F_ψ^{ext}	$F_{\alpha_R}^{ext}$	$F_{\alpha_L}^{ext}$	$F_{\gamma_1}^{ext}$	$F_{\gamma_2}^{ext}$
0.1 N.m	0.1 N.m	0.1 N.m	0.1 N.m	0.1 N.m
$t > 50$ s	$t > 58$ s	$t > 70$ s	$t > 80$ s	$t > 90$ s

Table 1: External disturbances.

	x	y	z	ψ
Adaptive	0.00215	0.00162	0.00009	0.77128
LQR	0.00033	0.00020	0.00002	0.77949
	f_R	f_L	τ_R	τ_L
Adaptive	7.14939	7.31984	0.51093	0.47581
LQR	5.00479	4.96759	0.38621	0.37646

Table 2: Performance indicators.

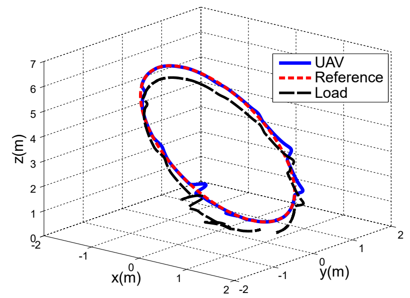

Fig. 2: Tree-dimensional trajectory - scenario 1.

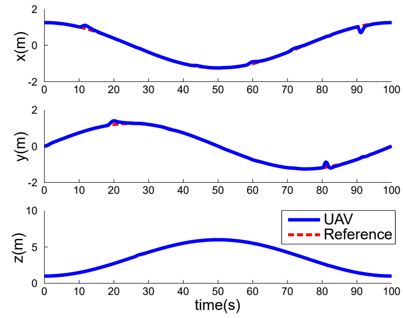

Fig. 3: Simulation of the states x, y, and z.

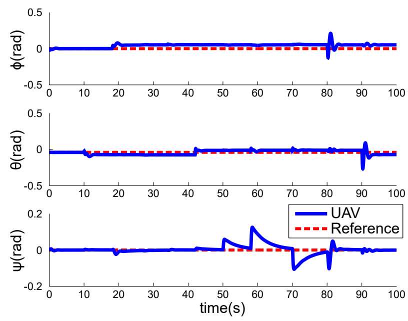

Fig. 4: Simulation of the states ϕ, θ, and ψ.

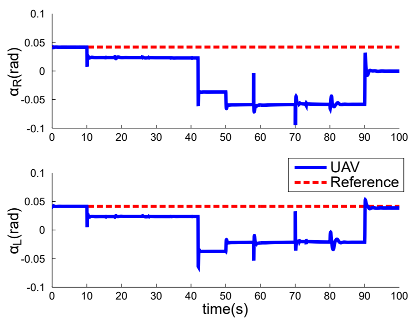

Fig. 5: Simulation of the states α_R and α_L.

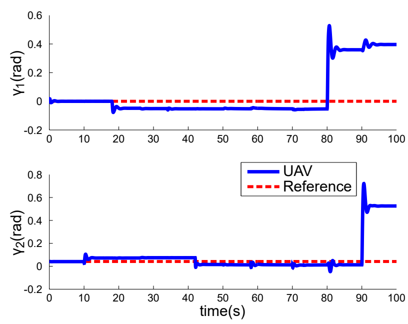

Fig. 6: Simulation of the states γ_1 and γ_2.

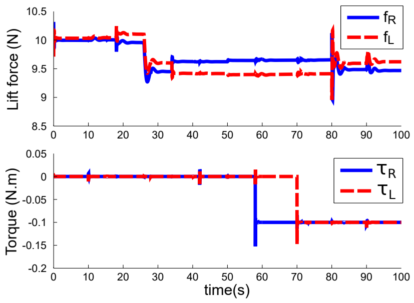

Fig. 7: Control input signals - scenario 1.

4.2 Scenario 2

This scenario simulates the system behavior when subject to accelerations around $\pm 2.5\ m/s^2$. Consider the reference trajectory given by $x = 3\cos((\pi/4)t)$, $y = 3\sin((\pi/4)t)$, $z = 4 - 4\cos((\pi/4)t)$, and $\psi = 0$. Fig. 8 and 9 show, respectively, the 3D trajectory and the control input applied to the system. Unlike the adaptive controller, in this scenario the LQR controller was not able to stabilize the system because it is designed for the nominal linearized system.

The adaptive controller presented in this work can be seen as a gain-scheduled controller able to ensure asymptotic stability over all operating region considered. Fig. 10 clearly shows how the optimization problem expressed in (21) schedule the system in order to obtain the best linear representation for the current realization.

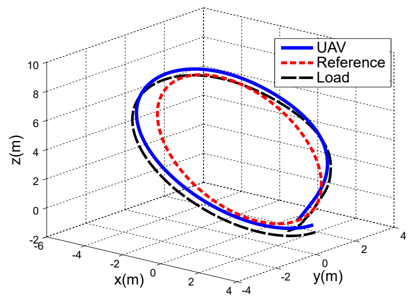

Fig. 8: Tree-dimensional trajectory - scenario 2.

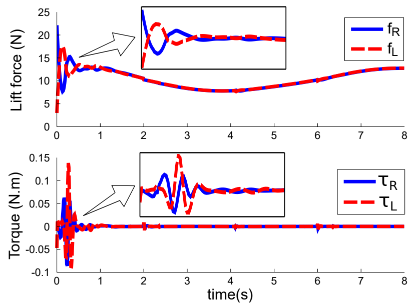

Fig. 9: Control input signals - scenario 2.

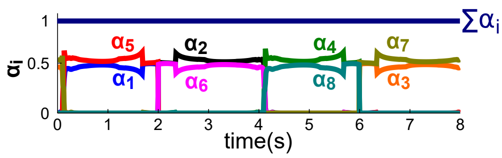

Fig. 10: Uncertain parameters α_i.

5 Conclusion

The simulation results show that the proposed adaptive controller is able to stabilize all states and reject external disturbances, ensuring the path tracking of the Tilt-rotor UAV carrying a suspended load. When comparing to a linear controller based on the nominal system, the proposed controller has worst performance near to the nominal model, i.e., for small accelerations. However when the system operates far from the nominal case, i.e., with high accelerations; the considered adaptive controller is better than controllers based on the nominal model because it increases the system domain of attraction allowing the system to work in a greater operational range.

Although this work addresses only the control problem of a Tilt-rotor UAV operating in rotary-wing flight mode, in the future the problem of transition between modes and path tracking in airplane mode will be considered to propose a complete solution to the load transportation problem.

ACKNOWLEDGMENT

The authors would like to thank the Brazilian research agencies CAPES, CNPq, and FAPEMIG for their financial support for the accomplishment of this work.

References

Álamo, T., Normey-Rico, J. E., Arahal, M., Marruedo, D. L. and Camacho, E. F. (2006). Introducing linear matrix inequalities in a control course, *Proc. of the 7th IFAC ACE*, pp. 205–210.

Almeida, M. M. and Raffo, G. V. (2015). Nonlinear control of a tiltrotor uav for load transportation, *Proc. of the IFAC Syroco*, IFAC, pp. 234–239.

Amiri, N., Ramirez-Serrano, A. and Davies, R. J. (2013). Integral backstepping control of an unconventional dual-fan unmanned aerial vehicle, *Journal of Intelligent & Robotic Systems* **69**(1-4): 147–159.

Donadel, R., Raffo, G. and Becker, L. (2014). Modeling and control of a tiltrotor uav for path tracking, *19th IFAC World Congress*, pp. 3839–3844.

Faust, A., Palunko, I., Cruz, P., Fierro, R. and Tapia, L. (2013). Learning swing-free trajectories for uavs with a suspended load, *IEEE ICRA*, pp. 4902–4909.

Gonzalez, R., Fiacchini, M., Alamo, T., Guzman, J. and Rodriguez, F. (2010). Adaptive control for a mobile robot under slip conditions using an lmi-based approach, *European Journal of Control* **16**(2): 144 – 155.

Johnson, M. and Grimble, M. (1987). Recent trends in linear optimal quadratic multivariable control system design, *Control Theory and Applications*, Vol. 134, pp. 53–71.

Papachristos, C., Alexis, K. and Tzes, A. (2013). Model predictive hovering-translation control of an unmanned tri-tiltrotor, *IEEE ICRA*, pp. 5425–5432.

Sreenath, K., Michael, N. and Kumar, V. (2013). Trajectory generation and control of a quadrotor with a cable-suspended load-a differentially-flat hybrid system, *IEEE ICRA*, pp. 4888–4895.